taken into account.

The data reported in [1] seem, therefore, to indicate that the inclusions are pure or almost pure magnesioferrite, with a nickel content of not more than a few per cent.

References

1. A. O. TOOKE, *J. Mater. Sci.* **10** (1975) 1830.
2. R. ENGIN and A. G. FITZGERALD, *ibid* **9** (1974) 169.
3. K. J. STANDLEY, "Oxide Magnetic Materials" (Oxford University Press, London, 1972).
4. W. H. VON AULOCK, ed., "Handbook of Ferrite Materials" (Academic Press, New York, 1965).
5. T. OKAMURA, *Sci. Repts. Res. Inst. Tohoku Univ.* **A6** (1954) 89.
6. K. I. ARAI and N. TSUYA, *J. Phys. Chem. Solids* **34** (1973) 431.

Received 30 December 1975
and accepted 6 January 1976

RONALDO SERGIO DE BIASI
Seção de Ciência dos Materiais
Instituto Militar de Engenharia
Urca, Rio de Janeiro, Brazil

Acoustic emisison from microcracks during sliding contact

Microcracks may be readily formed in brittle solids under comparatively small normal forces by dragging an indenter, e.g. a hard particle, across the surface; this process is responsible for most of surface damage and resultant strength degradation of brittle materials [1–5]. Thus "scratch resistance" is an important mechanical property which provides a useful figure of merit for assessing material response to many damage and wear situations. The physical significance of scratch resistance has been examined through a variety of contrived scratch systems, one in particular, the fixed spherical indenter on a smooth plane surface has been widely studied both theoretically and experimentally [6–8]. A typical system is shown schematically in Fig. 1 and a resultant set of crescent shaped microcracks formed in the wake of a sliding sphere on a polished glass surface is shown in Fig. 2.

One of the experimental difficulties associated with scratch tests has traditionally been in characterizing the intensity of the scratch. The number of microcracks, or crack density, constitutes a reasonably measurable parameter, but often involves tedious and time consuming measurements from optical observations. Wilshaw and Rothwell [9] attempted to measure the individual microcracks as they formed, by detecting and autographically recording the number and intensity of the stress waves emitted during unstable crack extension. The current study examines the relationship between the size and density of the microcracks and the recorded emissions in greater detail than before; a significant reduction

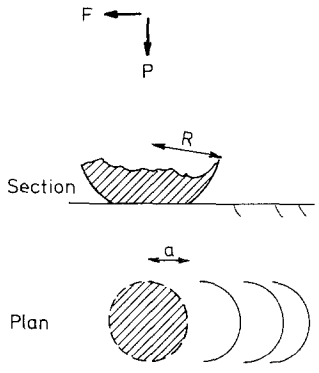

Figure 1 Diagram of a typical spherical sliding system, together with resultant microcracks. Normal load on the indenter, P, load on indenter parallel to surface, F, radius of indenter, R, radius of contact circle, a. Direction of indenter travel: from right to left.

in the emission strength with increasing microcrack density is observed and a physical explanation is provided.

The important variables involved in microcrack formation are illustrated schematically in Fig. 1. For a specific material with a uniform surface flaw size density distribution the fracture behaviour is determined by the contact stress field which, in turn, is governed by the applied load P on the indenter, the coefficient of sliding friction μ_K, the radius R of the indenter and the elastic properties of the indenter and work-piece (specimen). Surface roughness may also be an important parameter affecting μ_K, although in the present work this was not an important consideration since polished surfaces only were used. The experiments were carried out on mechanically polished blocks (50 m × 100 mm × 10 mm) of soda-lime-silica glass in a laboratory air atmosphere (25%

© *1976 Chapman and Hall Ltd. Printed in Great Britain.*

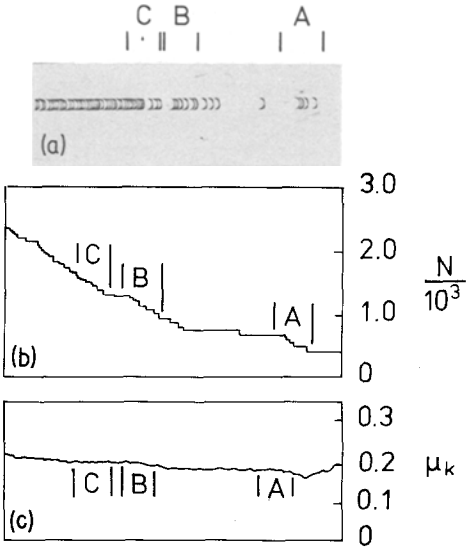

Figure 2 Typical set of crescent shaped microcracks formed in the wake of a sliding indenter. The corresponding cumulative emission count, N, and dynamic coefficient of friction, μ_K, are also shown. Direction of indenter travel: from right to left.

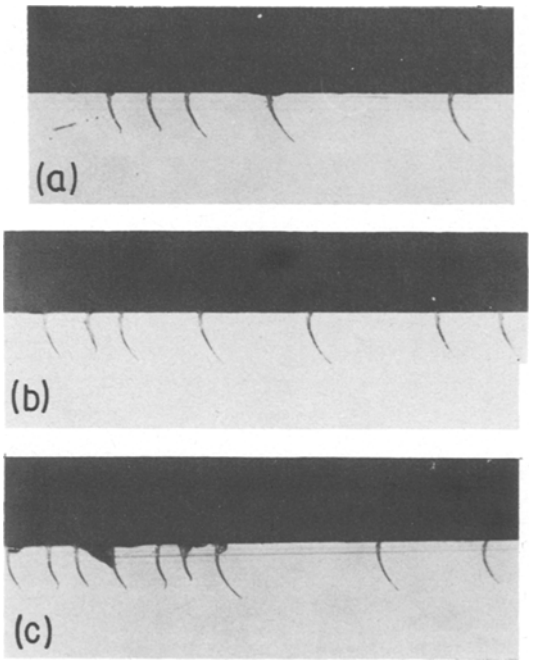

Figure 3 Enlarged vertical sections of the sliding trace shown in Fig. 2a. A, B and C above correspond to the regions so identified in Fig. 2. Direction of indenter travel: from right to left.

r.h.). The sliding track shown in Fig. 2 was obtained using a 2.0 mm radius tungsten carbide sphere under a normal force of 50 N with a relative sliding velocity of 4×10^{-5} m sec^{-1}.

The crack detection and analysing equipment are described elsewhere [10], for the present purposes it is sufficient to note that the mechanical/electrical conversion is effected using a piezoelectric transducer, and the signal strength measured using the ringdown count method [11]. The transducer was acoustically coupled to the specimen block through a thin layer of vacuum grease. Selected regions of the scratches were sectioned vertically along the axis of sliding, and after grinding and polishing the individual microcracks were revealed during a 30 sec etch in 5% HF.

A plan view of part of a sliding track is shown in Fig. 2a along with the corresponding cumulative acoustic emission trace (Fig. 2b) and associated coefficient of friction record (Fig. 2c). Vertical sections of selected regions of this trace are shown in Fig. 3. We note that the microcrack density increases from right to left; This is probably due to a correspondingly small but significant increase in the coefficient of friction over the length of the track. The random distribution of microcracks over the length to some extent the surface flaw size distribution which provides the microcrack.

Three aspects of the cumulative emission trace (Fig. 2b) are worth nothing: emission pulses may be identified with microcracks; there is no detectable emission from frictional processes at the contact interface; and the strength of the emission per crack is variable. We identify three regions of the track, A, B and C within which there is a variation in the microcrack density to amplify this last point. From the plan view in Fig. 2 and the sections in Fig. 3, the decrease in the strength of the emission signal corresponds to a decrease in microcrack length associated with an increase in microcrack density. We shall propose an explanation of this phenomenon using indentation fracture mechanics.

The maximum principal surface stress, σ_{11}, due to sliding spherical contact on an elastic half-space, is distributed on the axis of sliding as shown in Fig. 4a, for $\mu_K = 0.25$ (after Hamilton and Goodman [12]. The maximum tensile stress occurs on the periphery of the contact circle

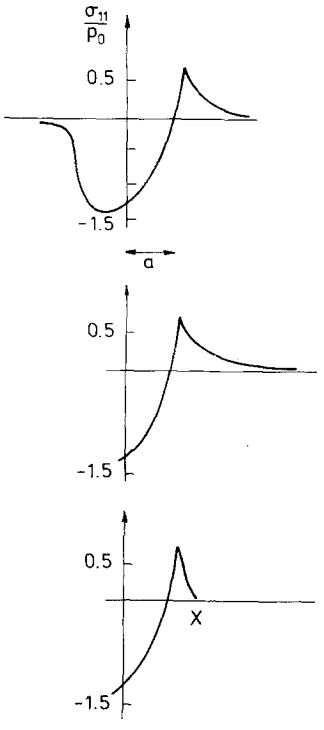

Figure 4 (a) The principal surface stress field, σ_{11}, normalized by the mean indenter contact pressure, p_0 (after Hamilton and Goodman [12]). (b) The surface stress field controlling crack growth for initial crack extension. (c) Probable surface stress field controlling subsequent crack growth after formation of initial crack at position X. Direction of indenter travel: from right to left.

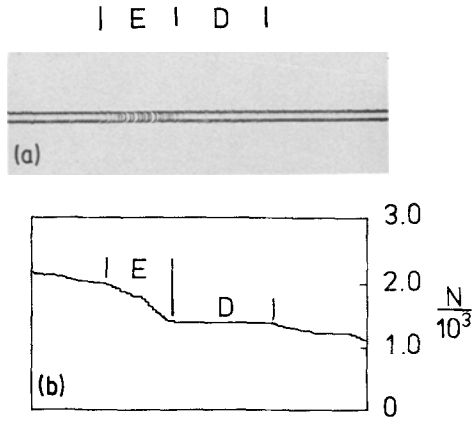

Figure 5 Cumulative emission count, N, together with corresponding high crack density sliding track. Direction of indenter travel: from right to left.

behind the sliding sphere. Microcracks tend to extend from this location whenever a surface flaw is critically stressed according to the Griffith equation (in practice a more complex relationship is necessary to account for the stress gradient on the nucleating flaw but in the interests of simplicity we shall not pursue this aspect further). In the absence of any other surface damage the initial crack forms in the undisturbed Hertzian stress field (Fig. 4b). Once a crack becomes unstable it extends away from the surface, emitting a stress wave, and relaxing the stresses in the vicinity of the stressfree surfaces created by the crack. If a second crack is subsequently extended within the sphere of influence of the first, it tends to extend a shorter distance due to the decrease in strain energy release rate caused by the stress relaxation (Fig. 4c). Apparently, the range of influence of the stress-free crack surface extends approximately one contact circle diameter according to our observations and measurements. At this stage we can only offer a qualitative explanation of this effect. For the relatively simpler case of cracking due to normal indentation we have established a quantitative relationship between the amount of crack extension and the associated intensity of the emitted stress waves [10]. In the present case, however, we have no quantitative understanding of the way in which the sliding contact stress field is modified by the presence of stress-free surfaces. Until such information becomes available we cannot proceed to quantify this effect. The above phenomena has important implications in the application of acoustic detection techniques to instrumenting scratch tests. As the crack density increases the size of the individual microcrack decreases until eventually it may becomes acoustically undetected. An example of this behaviour is shown in Fig. 5 in which a section of an overall high crack density scratch is presented. The lowest crack density occurs in region E corresponding to a slight reduction in μ_K. In this field the largest emission signal per crack is produced. The large crack density in region D comprises small microcracks which are acoustically undetected (Fig. 5b).

Acknowledgements

This work was carried out at The Materials Science Laboratories of The University of Sussex. Finan-

cial support was provided by The British Glass Industries Research Association, Sheffield and United Glass Ltd, St. Albans.

References

1. J. A. GREENWOOD and J. H. TRIPP, *J. Appl. Mech.* **34** (1967) 153.
2. B. LAWN and R.WILSHAW, *J. Mater. Sci.* **10** (1975) 1049.
3. G. M. CRIMES, *Ph.D. Thesis, University of Sussex* (1973).
4. S. J. SCHNEIDER and R. W. RICE, EDS., The Sciences of Ceramic machining and surface finishing Symposium proceedings (N.B.S. Special Publication 348, 1972).
5. S. M. WIEDERHORN and D. E. ROBERTS, *Wear* **32** (1975) 51.
6. B. R. LAWN, *Proc. Roy. Soc.* **A229** (1967) 307.
7. B. HAMILTON and H. RAWSON, *J. Phys. D. Appl. Phys.* **3** (9) (1970) 40; 2 (2) (1969) 1784.
8. D. R. GILROY and W. HIRST, *Brit. J. Appl. Phys. (J. Phys. D)* **2**, sec. 2 (1969).
9. T. R. WILSHAW and R. ROTHWELL, *Nature, Phys. Sci.* **229** (1971) 155.
10. W. E. SWINDLEHURST and T. R. WILSHAW, *J. Mater. Sci.*, to be published.
11. B. J. BRINDLEY, J. HOLT and I. G. PALMER, *Non-Dest. Test. December* (1973) 229.
12. G. M. HAMILTON and L. E. GOODMAN, *J. Appl. Mech.* **33** (1966) 371.

Received 23 January
and accepted 8 February 1976

W.E. SWINDLEHURST
Atomenergikommissionens forsøgsanlaeg Risø, 4000 Roskilde, Denmark

T.R. WILSHAW
Effects Technology, Inc, 5383 Hollister Avenue, Santa Barbara, California, USA